Applied Surface Science 558 (2021) 149740

Contents lists available at ScienceDirect

Applied Surface Science

journal homepage: www.elsevier.com/locate/apsusc

Full Length Article

Application of surface-enhanced Raman scattering in rapid detection of dithiocarbamate pesticide residues in foods

Chao-Ming Tsen [a,b], Ching-Wei Yu [c], Sz-Ying Chen [b], Cheng-Li Lin [b], Chun-Yu Chuang [a,*]

[a] Department of Biomedical Engineering and Environmental Sciences, National Tsing Hua University, 101, Sec. 2, Kuang-Fu Rd., Hsinchu 30013, Taiwan
[b] Residue Control Division, Agricultural Chemicals and Toxic Substances Research Institute, Council of Agriculture, Executive Yuan, No.11, Guangming Rd., Wufong 41358, Taichung, Taiwan
[c] Phansco Co., Ltd., 3F, No. 49, Lane 2, Section 2, Kuang-Fu Rd., 30071, Taiwan

ARTICLE INFO

Keywords:
Surface-enhanced Raman spectroscopy (SERS)
Dithiocarbamates (DTCs)
Glancing angle deposition (GLAD)
Alloyed nanorods
Carbon disulfide (CS_2)

ABSTRACT

Dithiocarbamates (DTCs) are a group of fungicides with various toxicities, and are widely used in agriculture. Currently, most of the official DTC detection methods cannot identify residues of individual DTCs, such as dimethyldithiocarbamates (DMDCs), ethylene-bis-dithiocarbamates (EBDCs) and propylene-bis-dithiocarbamates (PBDCs), on crops. Surface-enhanced Raman scattering (SERS) provides fingerprint recognition from the scattering spectra of molecular vibrations, and it has excellent potential as a primary qualitative screening tool. In this study, glancing angle deposition (GLAD) was used to fabricate SERS substrates with Ag@Au alloyed nanorods to provide cost-effective and rapid detection, and an optimal procedure for extracting DTC residues on the surface of crops was proposed. This study verified that under ordinary Raman spectroscopy conditions (excitation light, 785 nm; power, 20 mW; and integration, 3 min), extraction with tepid water and the addition of 0.1% sodium chloride can enable the detection of thiram (a DMDC), propineb (a PBDC) and mancozeb (an EBDC) on crops at trace concentrations of 0.05, 0.1 and 0.2 ppm, respectively, even on crops containing high levels of endogenous sulfides, such as cauliflower and white radish. Using the developed SERS-active substrate, qualitative and semi-quantitative results can be obtained by employing the specific characteristic peaks of the Raman scattering patterns to distinguish three types of DTCs. The method proposed in this study offers the advantages of simple operation, few consumables, high safety, and no interference from the matrix. Hence, this study provides an auxiliary approach for DTC detection.

1. Introduction

Dithiocarbamates (DTCs) are a group of compounds containing disulfide substituents and are used as pesticides. As contact broad-spectrum bactericides, DTCs are effective against more than 400 types of pathogens and have been widely applied to more than 70 types of crops, with an annual global consumption of more than 35,000 tons. Depending on the carbon chain structure of the molecule, DTCs can be divided into three major types: (1) dimethyldithiocarbamates (DMDCs), such as thiram and ferbam; (2) ethylene-bis-dithiocarbamates (EBDCs), such as mancozeb, maneb, and mitram; and (3) propylene-bis-dithiocarbamates (PBDCs), such as propineb. Generally, DTCs are not particularly toxic, and they are sprayed directly onto the surface of crops; they can be easily removed by washing with water. However, DMDCs are moderately toxic bactericides, and their toxicity can be significantly enhanced when heavy metal ions are included and cause poisoning through dietary exposure or skin contact. The metabolite of mancozeb and zineb (both EBDCs) is ethylene thiourea (ETU), which has been classified as a Group 3 carcinogen by the International Agency for Research on Cancer (IARC) [1]. Although the carcinogenicity of ETU to humans is still uncertain, it has been found to be carcinogenic and teratogenic in animal experiments, causing thyroid follicular cell carcinoma, anterior pituitary tumor, and liver cancer in mice and thyroid epithelial cancer in rats [2]. The metabolite of propineb (a PBDC) is propylene thiourea (PTU). An animal study revealed that long-term consumption of ETU or PTU leads to adverse effects on abnormal thyroid and embryo malformation [3].

Since individual DTCs vary in toxicity, the assessment of exposure to individual DTCs according to each of their toxicities would more accurately reflect the actual risk that consumers face [4]. To precisely

* Corresponding author.
E-mail address: cychuang@mx.nthu.edu.tw (C.-Y. Chuang).

https://doi.org/10.1016/j.apsusc.2021.149740
Received 14 January 2021; Received in revised form 24 March 2021; Accepted 1 April 2021
Available online 25 April 2021

determine the level of exposure, a method that is capable of distinguishing the content of individual DTCs is necessary. For this purpose, the European Union stipulated maximal residue level (MRL) standards for DTCs in 2007, which indicated that specific methods must be applied to individually determine residual propineb, thiram, and ziram on foods [5]. However, DTCs are insoluble in most solvents, and their stability is dependent on the oxygen content, humidity, temperature, and pH value [3]. Therefore, it is difficult to directly determine the content of undegraded DTCs. At present, many countries and international organizations use CS_2 content to represent total DTC residue levels in agricultural products. The presented universal method is to determine the CS_2 content by headspace gas chromatography after the reduction reaction of the sample crops. The first method was proposed on the basis of the principle that DTCs are hydrolyzed to release CS_2 in an acidic $SnCl_2$ solution [6]. Then, the released CS_2 can be determined using various instruments, such as spectrophotometry [7], gas chromatography-flame photometric detector (GC-FPD) analysis [8], gas chromatography-mass spectrometry (GC–MS) [9], and flow injection spectrophotometry [10]. Since carbamate pesticides and organophosphorus pesticides can compete with acetylcholine for the active site of acetylcholinesterase (AchE), enzyme-based electrochemical and fluorometric approaches have emerged as powerful pesticide screening assays [11-13] and have great potential for detecting pesticides with thiocarbamate, which is the sulfur analogue of carbamate.

Although some of these methods are quick and easy and offer short analytical times, simple operation, and high detection sensitivity, they cannot be used to determine the individual contents of various types of DTCs. Moreover, certain plant matrices generate CS_2 during the process of degradation or decomposition. Some crops also form CS_2 from endogenous sulfides through reduction reactions. Therefore, the high content of sulfide in crops (e.g., cruciferous crops (cauliflower and white radish), mushrooms, onion, garlic, and chives) would yield false-positive results in the above CS_2 determination methods [14].

Surface-enhanced Raman scattering (SERS) provides the benefits of quick analysis, excellent sensitivity to detect chemical molecules down to ultratrace levels and unique information on molecular vibrational fingerprints. SERS has gradually become a promising tool in applications in food safety, environmental monitoring, and life science [15-18]. Although numerous studies have investigated the application of SERS to detect pesticides in fruits and vegetables, thiram has almost always been used as the target substance for DTC detection [19]. Few studies have proposed the application of SERS for the detection of EBDCs and PBDCs, even though these DTCs present higher risks than thiram to human health. One credible reason for this paucity of studies is that the detection limits of EBDCs and PBDCs by SERS are almost above the current MRL requirements ($\sim 10^{-7}$ M). A previous study using SERS to detect mancozeb achieved a sensitivity of only trace amounts of 10^{-6} M [20], and in another report, in which Au and Ag nanostructures on paper were prepared as substrates for SERS to detect mancozeb, the method showed poor sensitivity (1.28×10^{-3} M) [21]. To our knowledge, aside from DMDCs and EBDCs, no studies have been conducted using SERS for propineb, a type of PBDC.

With the prosperous development of SERS substrate materials, numerous SERS-based methods facilitate real-time on-site analysis [22]. SERS applications have been reported with two nanostructured systems: colloidal dispersions of metal particles and nanostructured metal films [23-25]. Compared with colloidal systems, the nanostructured film approach provides more advantages for SERS substrates, such as portability, robustness, and compatibility with a wider variety of substrates. However, due to the complex preparation process and high purity requirements, the use of metal thin films as a rapid detection method is hindered. As part of the physical vapor deposition (PVD) process for creating coatings of pure metals, metallic alloys and ceramics, glancing angle deposition (GLAD) is an ideal method for preparing nanomaterials [26]. Nanostructures with specific morphologies and excellent properties can be fabricated that are suitable for preparing highly sensitive SERS substrates. One of the novel materials used as a SERS substrate is Ag/Au bimetallic nanoalloy, which combines the benefits of the surface stable properties of Au with the scattering enhancement properties of Ag [27-29]. Such nanostructures offer the advantages of easy control, broad applicability, low operation pollution and good stability and repeatability at large scale for producing SERS-active substrates [30-32]. Using GLAD to fabricate Ag@Au bimetallic nanostructures can achieve SERS substrates with more effective hot spots at low cost.

DTCs are not included in the routine analysis of multi-pesticide residues in agricultural products because they cannot be determined by general procedures such as quick, easy, cheap, effective, rugged, and safe (QuEChERS) methods. Although mass spectrometry can distinguish the different types of DTCs, it remains a challenge to accurately quantify DTCs using LC-MS/MS for routine analysis since DTC standards as calibration standards are unstable. In addition, the current analytical method to determine DTC residues, which is based mainly on CS_2 level, has identification defects and a high false-positive rate. On the strengths of high sensitivity and rapid quantification, SERS has potential as a screening tool for detecting DTC residues. Thus, this study was aimed at developing a simple approach that uses an alloyed SERS substrate accompanied with a rapid extraction process to detect DTC residues in vegetables and fruits, and thereby overcome the difficulties faced by current DTC detection methods.

2. Experimental

2.1. Reference standard and chemical reagent

Reagents included sodium chloride (special grade), deionized water (resistivity $\geq$ 18 MΩcm at 25 °C), pesticide reference standards (standard grade: 99.8% thiram, Sigma-Aldrich., USA), 99.8% propineb (Sigma-Aldrich), and 89.7% maneb (Sigma-Aldrich). The formulated agro-pesticides used for testing were mancozeb, (80%, wettable powder (WP), Sinon Corp., Taiwan), propineb (70%, WP, Sinon Corp., Taiwan), thiram (80%, WP, Taminco Corp., USA), and metiram (80%, water-dispersible granules, BASF Corp., Germany). A stock solution of standard pesticide was prepared by dissolving 5 mg of the pesticide reference standard in 100 mL of deionized water with sonication for 5 min. Subsequently, the standard stock solution was diluted with deionized water to prepare each desired concentration of standard samples. The 1000 mg/L NaCl solution was prepared by dissolving 4 mg of NaCl in 4 mL of deionized water and storing at −4°C after mixing.

2.2. Fabrication of a Ag@Au bimetallic substrate for SERS measurement

This nanostructure required an electron gun system for electroplating and the self-rotating mechanism of the substrate to carve nanopillars. During the electroplating process, the substrate stage and the evaporation source were set at an angle of 89°, and the substrate simultaneously rotated around the normal line to grow each metal nanocolumn with different diameter/pore distributions. Ag nanocolumn films with a mass thickness of 230 nm were prepared on a commercial electronic grade silicon wafer (p-type) in an electron beam evaporator (Temescal Model 294 E-Beam Source, Ferrotec Corp., Santa Clara, CA). During film deposition by Ag nanocolumns and Au nanoparticles, the background pressure was 10^{-6} Torr. The Raman system was equipped with a 785-nm laser line and charge-coupled device (CCD) detector, which collected inelastically scattered radiation. All measurements were performed in an effective area greater than 2.2 mm^2, the surface was able to withstand 20 mW laser power (4× focusing objective lens), and the SERS spectra were collected within an integration time of 6 s.

2.3. Preparation and evaluation of the incurred samples

Equal amounts of romaine lettuce and broccoli (30 g) were immersed in an aqueous solution containing 40 mg/L DTC pesticides in water to

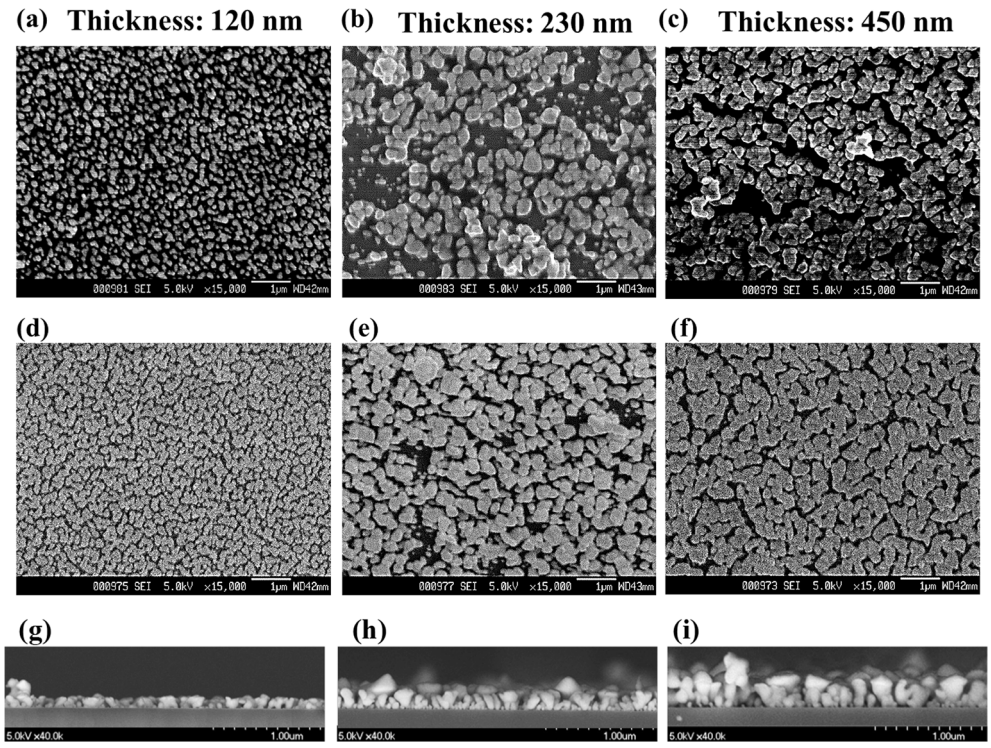

Fig. 1. Microstructure of nanorods. The top view of nanorod microstructure corresponding to three different thicknesses of films, (a) 120 nm, (b) 230 nm, and (c) 450 nm, was observed by SEM. (d)-(f) Images of nanorods dropped with the formulation thiram (1.0 mg/L). The cross-section images in (g)-(i) correspond to the films in (d)-(f).

ensure even contact of pesticide molecules with the plants. After 15 min, the plants were removed from the solution and placed outdoors in sunlight for 2 h to simulate a farm environment. Three to five samples of each crop were prepared; the content of CS_2 in the homogenized samples was determined using GC-FPD, and the DTC content in the samples after rinsing was detected by SERS. The concentration of DTC was obtained by multiplying the conversion factor by the CS_2 concentration determined from the homogenized samples. The recovery ratio of surface extraction was then calculated. For a fixed volume of solution in a flask, one molecule of thiram (M.W. 240) generated two molecules of CS_2 (M. W. 76) by reaction with a reducing agent. The following formula was used to determine that the concentration of thiram was 1.58-fold that of CS_2, which served as the conversion factor for the concentration of thiram in terms of CS_2:

$$\frac{[Thiram] \times V}{240} : \frac{[CS2] \times V}{76} = 1 : 2$$

$$[Thiram] = 1.58 \times [CS_2] \quad (2)$$

The same calculation method revealed that the conversion factors of propineb and mancozeb were 1.92 and 1.78, respectively [33].

2.4. Estimating the extraction efficiency

A clean part of the sample was subjected to extraction and maintained in its original state (i.e., not broken or ground). Any sand or dirt found on the surface was brushed off. The specimen was then placed in a beaker (or a stainless steel plate), wetted with an amount of deionized water whose weight was equivalent to one-third of the specimen weight, and then rinsed 5–8 times; the wash fluid was collected and served as the extraction solution of the specimen. Next, 10 μL of the specimen solution was placed in a 0.2-mL centrifuge tube, evenly mixed with 10 μL of 0.1% NaCl solution, and allowed to settle for 5 min.

The efficiency of extraction and recovery of DTCs in crops through a surface rinse method was evaluated. Samples of equal concentrations were prepared with two types of crops: romaine lettuce and broccoli. Romaine lettuce contains a low content of endogenous sulfur, enabling accurate quantification of CS_2, for which the limit of detection (LOD) by GC-FPD was 0.1 ppm. In contrast, broccoli contains a higher content of endogenous sulfur, which interferes with the quantification of CS_2 if traditional detection methods are used. The blank control check group (CK) of the broccoli samples was washed with clean running water prior to beginning the experiment. Five CK samples were collected to determine CS_2 using GC-FPD, and the other 5 CK samples were analysed by SERS. The incurred samples of three types of formulated DTCs were prepared by dilution with water to 40 ppm and 80 ppm. Water-washed romaine lettuce was soaked in DTC (aq) for 10 min and then placed outdoors under sunlight for 2 h. A 30 g of plant sample was prepared for analysis.

All of the DTC molecules were assumed to be dispersed across the surfaces of the vegetable samples. Therefore, if we rinse out all the DTC molecules with clean water whose weight was equivalent to one-third that of the samples, a threefold concentrated extract of the DTC solution was obtained. Therefore, the concentration of DTC was first quantified according to the height of the main characteristic peak in the SERS spectrum. Then, the CS_2 concentration of the surface extract (*Cs*) was obtained using the conversion factor and multiplying the concentration value by one-third. Comparing the CS_2 concentration of the homogenized extract (*Cm*) via GC-FPD, the recovery ratio R of surface extraction was defined as follows:

$$R(\%) = \frac{C_S}{C_m} \quad (3)$$

3. Results and discussion

3.1. Characteristics of the SERS substrate

The three nano-silver columns with different film thicknesses (120, 230, and 450 nm) were observed under SEM (Fig. 1 (a)-(c)), and top-

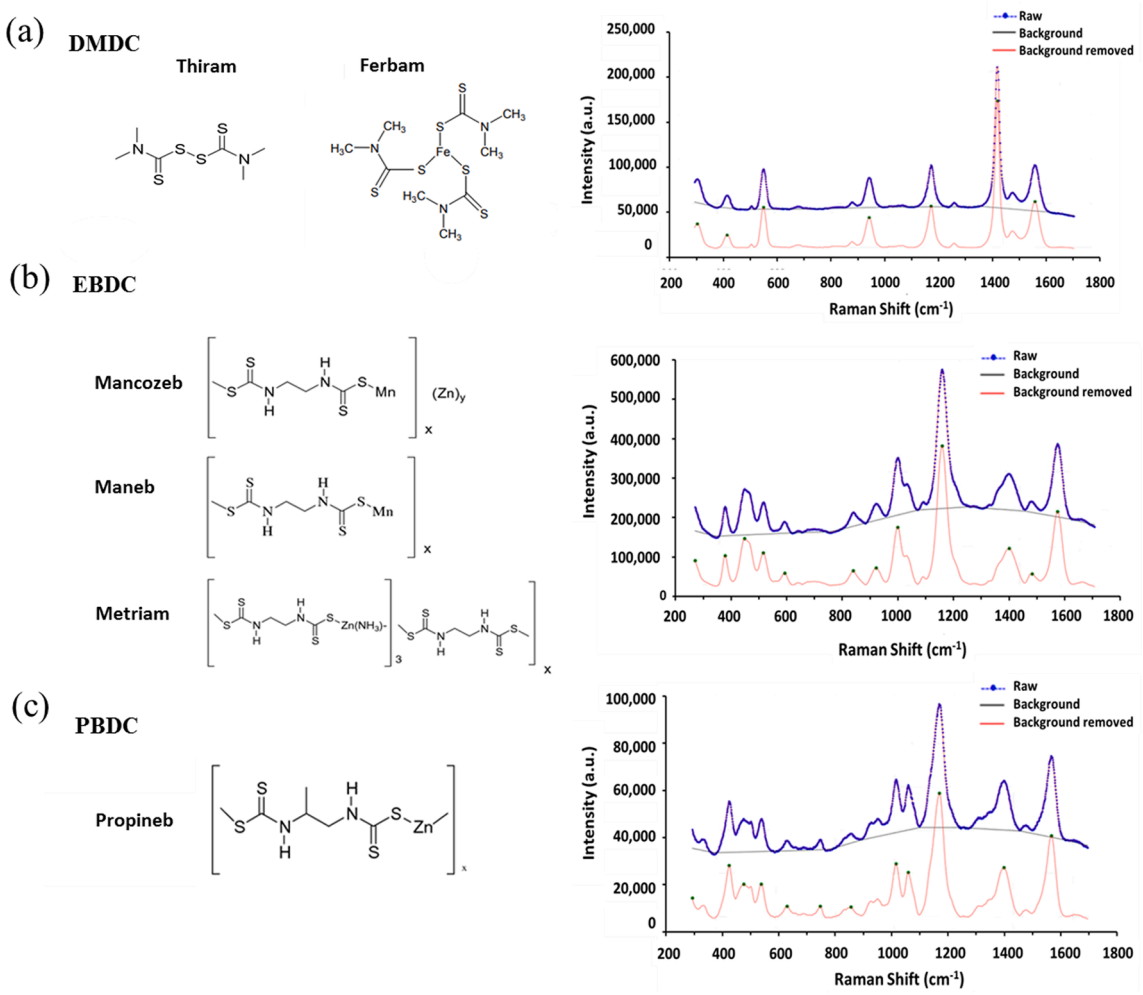

Fig. 2. SERS spectra of three DTCs. The six dithiocarbamate fungicides were divided into three groups of DTCs according to their carbon–sulfur chain structure. SERS spectra of three DTC reference standards (blue curve) with normalization (red curve): (a) thiram (0.2 mg/L), (b) mancozeb (1 mg/L) and (c) propineb (1 mg/L).

view and cross-section images of these nanorod substrates dropped with formulated thiram (1.0 mg/L) were shown in Fig. 1 (d)-(i). The diameter of the nanometal column increased with increasing film thickness. Therefore, the distance between the alloyed nanorods easily approached each other, thereby resulting in a larger gap. Thicker films had more gaps and more hot spots while increasing the strength of the SERS signal. In this study, we prepared silver nanopillars (AgNPs) with a diameter of 150–250 nm and a height of 230 nm on Si substrates. The chosen height was close to the optimal height according to the finding of a previous study [34]. We further used AgNPs to fabricate an optimally enhanced alloyed film sensor, which should be able to detect at low concentrations and possess a longer shelf life. Compared with the 230-nm AgNP chips without an Au film, the main characteristic peak (1381 cm^{-1}) of the chip with the 230-nm column stacked AgNPs plated with a 5-nm Au nanoparticle outer layer exhibited a 7 times stronger signal intensity at the level of 1 ppm thiram (data not shown).

It is well known that the outer layer of metal nanomaterials controls the interaction with light because the electromagnetic fields greatly decay inside the metals. The plasmonic efficiency and electromagnetic enhancement effect of silver film are greater than those of Au film because Au exhibits less free-electron behaviour than Ag [35]. When the Au film is formed on the Ag surface, the strength of the local electrical field is significantly reduced. Hence, in theory, the enhanced ability of the Ag@Au bimetallic nanoalloy structures needs to be weaker than that of Ag slices, since the outer metal of this alloyed structure is Au. However, the enhancement phenomenon of our Ag@Au film was inconsistent with the above deduction. We inferred that the enhancement of the Raman signal mainly originated from local field enhancement, which arose due to two aspects, namely, hot spots and plasmonic mode coupling. Between the Ag@Au nanopillars, many hot spots were formed, leading to an enhanced electric field. Even though the Au ratio increase affects the SERS enhancement, a previous study indicated that the Ag-Au hetero-structure surface morphology and shape play more critical roles than the Au ratio in SERS [36].

Since AgNPs are not regular in rod arrays (Fig. S1), it is not easy to perform electromagnetic (EM) simulations. The number of molecules adsorbed between the rods is another factor that can be used to evaluate SERS enhancement. For AgNPs with a smaller porosity, fewer SERS molecules were adsorbed between the pores. However, the gap between the nanorods was small, and most of the EM field was located in the gaps. As the porosity of the NP array increased, the coupling between the plasmons in the gaps decreased, but the number of SERS molecules adsorbed in the gaps increased. When the plasmonic field reached the maximum for the interactions of SERS molecules adsorbed in the gaps as well as on the tips or edges, equilibrium existed at the optimal porosity.

3.2. SERS spectra of DTCs

The reference standards of DTCs were diluted to concentrations of 0.2 or 1.0 mg/L using acetonitrile. The Raman characteristic peaks (functional group bonds) of DTCs were shown in Fig. 2(a)-(c). Accordingly, the DTC spectra can be used to group the DTCs into three types

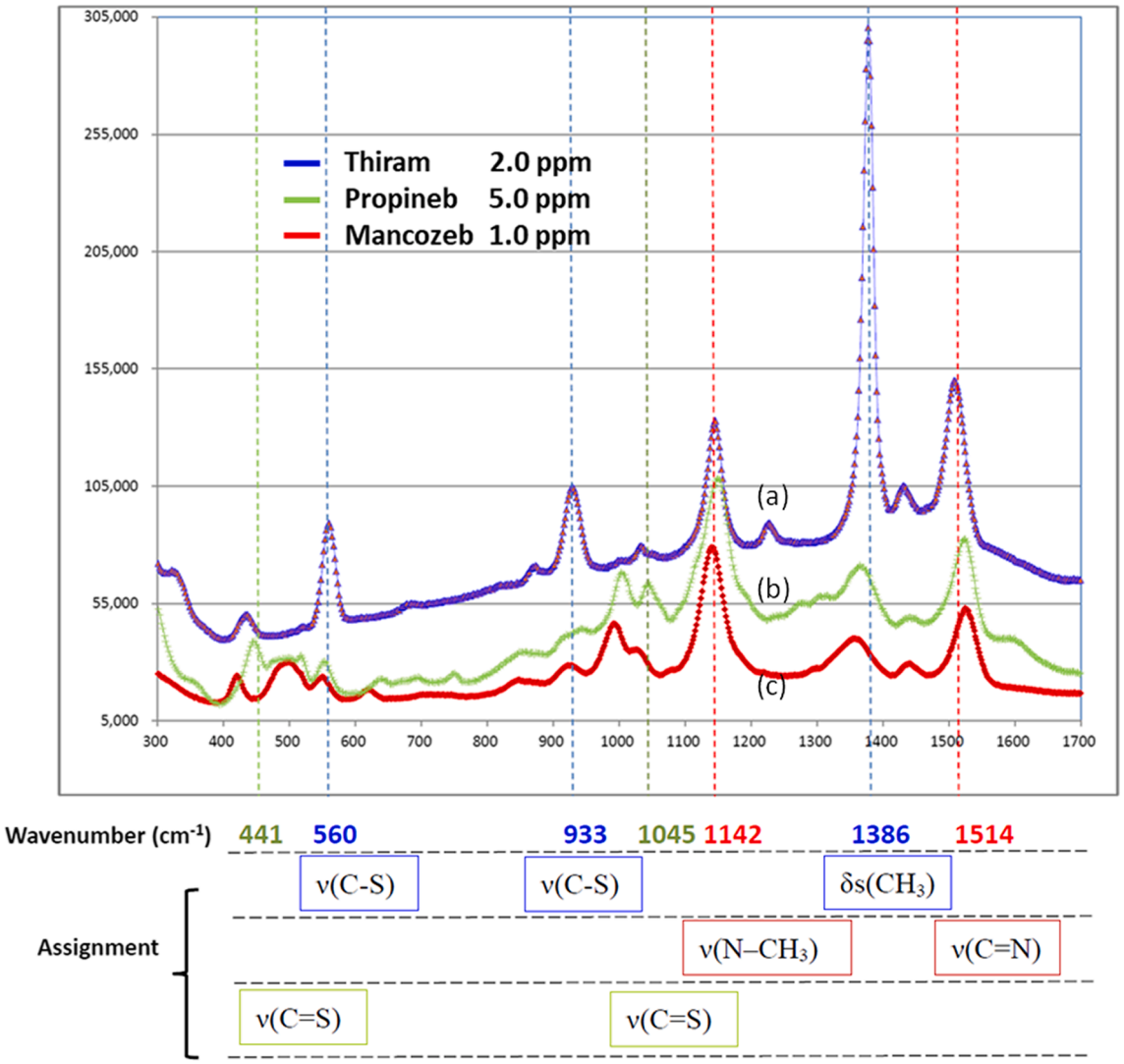

Fig. 3. The characteristic peaks of the three DTC structures in the SERS spectra and their corresponding bonding vibration wavenumbers. (a) thiram (2.0 mg/L), (b) propineb (5.0 mg/L) and (c) mancozeb (1.0 mg/L).

based on their structural formulas, namely, EBDCs, PBDCs, and DMDCs. Since SERS can acquire vibrational spectra of very dilute DTC fungicides, the characteristics of these substances can be studied for their natural chemical state by means of a vibration procedure. Based on the SERS spectra, the reason that these fungicides degraded upon interacting with the silver surface is attributed to the high affinity of the DTC moiety bound to the metal surface. DMDCs (such as thiram and ferbam) were cleaved at the disulfide bond to generate two DTC ions and interacted with the metal surface of the SERS substrate through two types of coordination complexes with different geometries: monodentate and bidentate forms.

3.2.1. *DMDC: thiram*

The SERS spectra of thiram showed a maximum intensity band at 1386 cm^{-1}, which corresponded to the symmetrical bending of methyl vibrations: $\delta s(CH_3)$. Other bands attributable to the methyl group at 1148 cm^{-1} corresponded to rocking $\rho(CH_3)$ and stretching $\nu(N–CH_3)$ motions. In the SERS spectra of EBDCs and PBDCs, due to the lack of symmetrically vibrating methyl groups, the intensity of the bending signal $\delta s(CH_3)$ at 1386 cm^{-1} was significantly reduced, and more shoulders appeared. The $\nu(C = N)$ band at 1514 cm^{-1} was highly correlated with the DTC bidentate complexes. Thus, for DTC compounds, the position of the band at approximately 1500 cm^{-1} can be used to estimate the strength of the ligand–metal interaction [29,37]. The thioureide tautomer must predominate over the DTC form (Fig. S2 (a)) and form bidentate complexes (Fig. S2(b)) due to the strong electronic attraction of the nitrogen electron lone pair to the metal. The appearance of the 1514 cm^{-1} line reflected enhancement of the ν(C–N) mode perpendicular to the Ag surface. Obviously, the polarizability of this mode is low and greatly enhanced after adsorption [38]. However, both EBDCs and PBDCs themselves chelated metal ions, so the polarizability of the C–N bonds did not change much regardless of whether they contacted the metal surface of SERS. Due to the presence of ethyl groups, ions cannot be completely adsorbed because of stereochemical constraints, and EBDC or PBDC anions are more likely to adsorb on the edge through sulfur groups [39]. If the nitrogen atom is bound to a metal centre, the ethyl group will be removed, which indicates that the C = N stretching frequency should decrease, as observed in the SERS spectra of alkenes. No such evidence was found in the SERS spectrum, and contrary evidence was indeed found, i.e., the peak of the C–N stretching mode was slightly shifted to a higher wavenumber (1533 cm^{-1}). Not only in DMDCs but also in EBDCs and PBDCs, the band observed at 560 cm^{-1} was assigned to ν(CSS) [21,40] and coupled with ν(S–S), which is attributed to disulfide cleavage occurring on the metal surface; other similar disulfide-containing molecules were also observed [41].

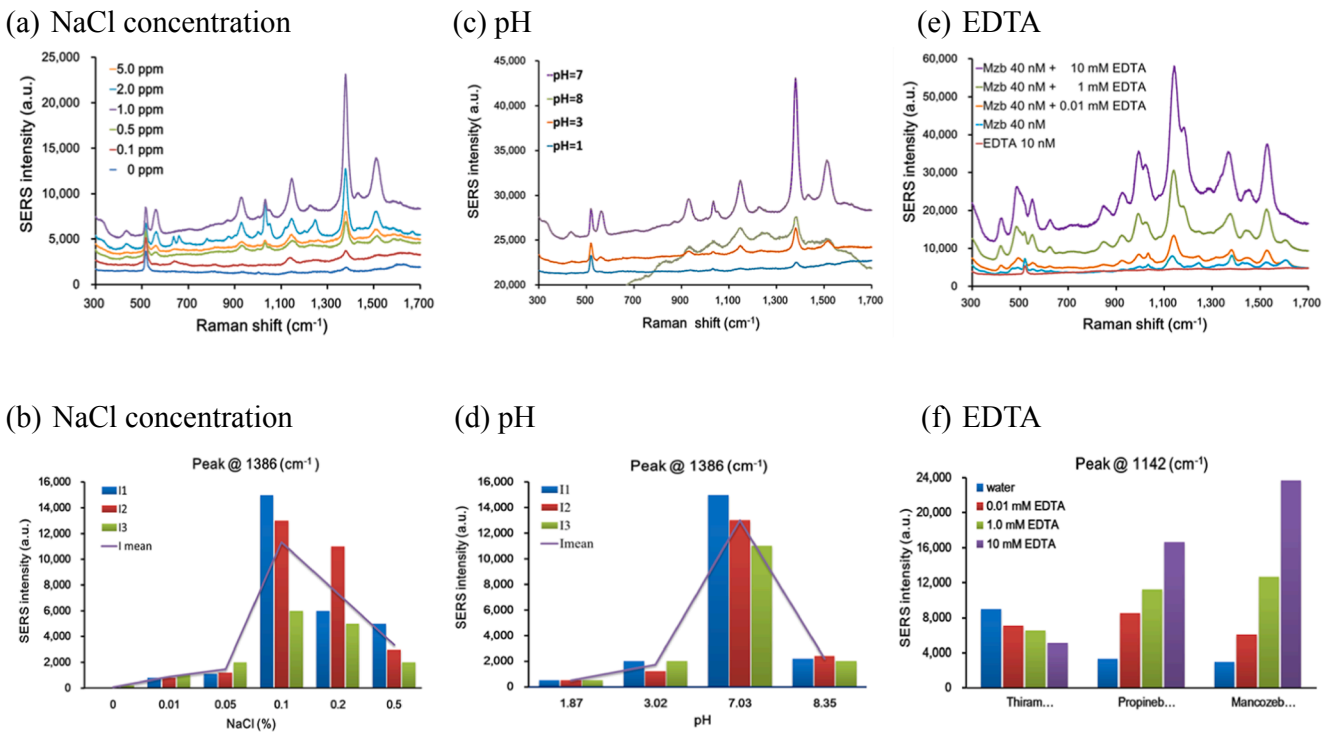

Fig. 4. Factors affecting the SERS signal intensity of the DTC reference standard. The DTC reference standard was dropped on a wafer of 230-nm thickness. The spectra and histogram of SERS signal intensity of thiram (1 ppm) in various concentrations of NaCl(aq) at pH 7 (a, b) or in 0.1% NaCl(aq) with various pH values (c, d). (e) SERS spectra of mancozeb in various concentrations of EDTA. (f) The SERS spectrum of elevated EDTA levels.

3.2.2. *EBDCs and PBDCs*

In addition, the band at 933 cm^{-1} corresponding to the ν(C–S) mode was characteristic of bidentate chelating complexes, and the other band observed at 1045 cm^{-1} was assigned to ν(C = S) modes. As a result, two ν(C = S) bands were observed at 1045 and 933 cm^{-1} in the SERS spectra of EBDC and PBDC. We inferred that both monodentate and bidentate silver complexes existed on the SERS surface (Fig. S2(b)), as previously reported by Bonati and Ugo [42]. Even in a previous study, a band at 1045 cm^{-1} was observed in the SERS spectrum of thiram [42], but in our study, the decreased intensity of this band may be attributed to the excellent binding efficiency of thiram on the SERS surface, with almost no free thiram ions. In other words, almost all DMDCs formed bidentate complexes with the SERS surface, and no ν(C = S) mode was observed. However, for EBDCs or PBDCs, even if one (CSS) moiety bound to the metal on the surface to form bidentate complexes, the other (CSS) moiety remained free, exhibiting ν(C–S) and ν(C = S) signals at 933 cm^{-1} and 1045 cm^{-1}, respectively.

Another band assigned to δ(CSS) appeared at 433 cm^{-1} in the SERS spectra of thiram. At high concentrations of thiram, the intensity of this band was very weak, while it was relatively obvious at low concentrations. This difference can be attributed to the reorientation of the adsorbent, which tended to interact with the metal through the bidentate binding mode. In the EBDC and PBDC spectra, the bending vibration wavenumbers of CSS shifted to 427 cm^{-1} and 441 cm^{-1}, respectively. These shifts may be attributed to change in the bond strength by the electron cloud density of adjacent nitrogen atoms, which indeed facilitated the process of clearly distinguishing EBDC from PBDC. Unlike the nitrogen atoms connected with two methyl groups on DMDC, the nitrogen atom of EBDC was connected to a hydrogen atom and an ethylenecarbamate group, while PBDC has two nitrogen atoms, one of which is bonded to a methyl group. Therefore, the (CSS) bending vibration frequencies between these three DTCs were different. Based on the electron induction effect, the methyl group on the PBDC molecule tended to donate electrons to generate a (C = S) form much more readily than the EBDC molecule, resulting in more intense vibration signals at 1045 cm^{-1} in the SERS spectrum of PBDC than EBDC, which is one of the important clues to discriminate these two types of DTCs. This qualitative SERS spectrum can be easily identified not only at high concentrations but also at low concentrations of 0.2 ppm.

From these qualitative inferences based on the SERS spectra, this study established a recognition procedure that can distinguish the six DTCs into three categories (Fig. 3). It can be preliminarily considered that the spectrum of each DTC at the positions of 1142, 1386 and 1514 cm^{-1} showed intense bands along with the following: (1) the intensity of the characteristic peak at 1386 cm^{-1} was higher than that at 1124 cm^{-1} and 1514 cm^{-1} as well as obvious peaks at 560 cm^{-1} and 933 cm^{-1}, which can be indicated as DMDC; (2) the peak height at 1386 cm^{-1} was lower than that at 1124 cm^{-1} and 1514 cm^{-1}, and accompanied by two less intense but clear peaks at 441 cm^{-1} and 1045 cm^{-1}, which indicated the existence of PBDC, and (3) the intensity at 386 cm^{-1} was lower than that at 1124 cm^{-1} and 1514 cm^{-1}, there was no obvious peak splitting from 1008 cm^{-1} at 1045 cm^{-1}, and some peak shifted to 422 cm^{-1}, which indicated that the compound was determined to be EBDC. To the best of our knowledge, this study is the first application of SERS to distinguish these three types of DTCs.

3.3. *Factors affecting the SERS intensity*

Previous studies have reported that some factors (e.g., NaCl concentration, pH value, mixing time, ethylenediaminetetraacetic acid (EDTA)) affect the intensity of Raman signals in the SERS spectrum [38]. NaCl is well known to cause plasma resonance at the SERS hot spot, enhancing the Raman scattering signals. Regarding the effects of various concentrations of NaCl solutions on the intensity of DTC signals, the SERS spectra of 1 ppm thiram mixed with 0.01%, 0.05%, 0.1%, 0.2%, and 0.5% NaCl solutions were shown in Fig. 4(a), and the intensities of the main characteristic peak (1381 ± 5 cm^{-1}) in NaCl(aq) at different concentrations were shown in Fig. 4(b). With no NaCl solution in the sample, the characteristic peak could not be detected. However, with increasing NaCl concentration, the signal intensity increased. When the

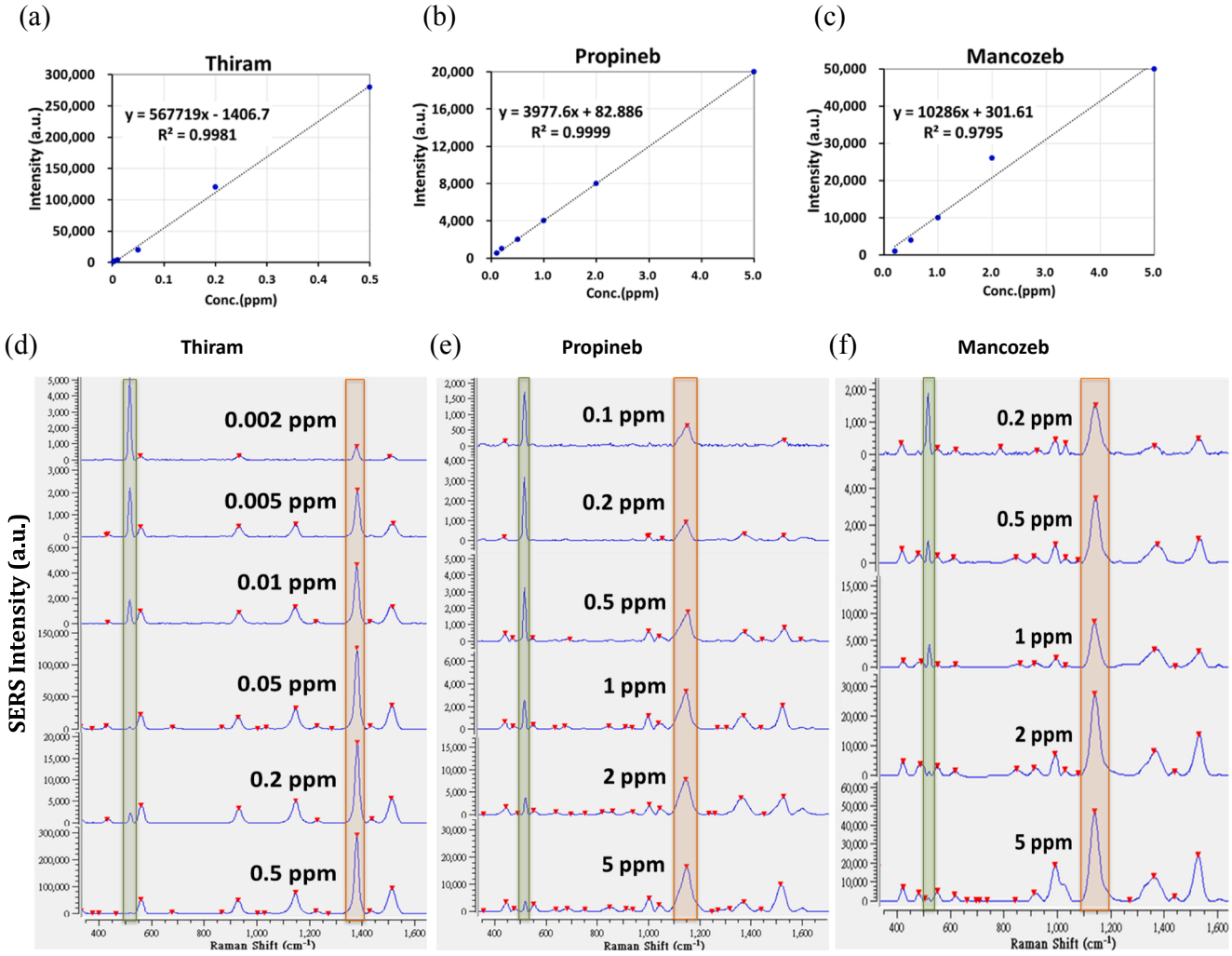

Fig. 5. The standard curve of different DTCs by concentrations. (a) thiram (2 ng/mL to 0.5 mg/L), (b) propineb (0.1 mg/L to 5 mg/L), and (c) mancozeb (0.2 mg/L to 5 mg/L). The vertical axis values for each point in the calibration curve represented the intensity of the normalized characteristic peak (orange band) of (d) thiram, (e) propineb, and (f) mancozeb from the raw spectrum (supplemented in Figure S3). The SERS substrate contributes the silicon line (Si/ SiO_2) at 520 cm (green band). ng/mL: ppb; mg/L: ppm.

NaCl concentration was 0.1%, the signal intensity reached its highest value and then gradually decreased as the NaCl concentration further increased. Positively charged Ag ions can be stabilized by Cl^- ions or other co-adsorbed species [38]. This enhancement may result from the positive charges induced by the coadsorbed chloride, followed by the interaction between thiram and the Ag surface. When a complex between the active site and a probe molecule forms, the amount of Cl^- ions adsorbed around Ag or Au stimulates the connected band. The results of this study suggest that two S atoms of the DTC molecule bind on the metal surface and that the vibration of the metal adsorbate was affected by the halide ions at the interface near the metal surface, forming a stable complex.

Under the condition of 0.1% NaCl(aq), we further evaluated the optimal pH value for determining the 1 ppm thiram solutions with 1% formic acid (pH = 1.87), 0.01% formic acid (pH = 3.02), H_2O (pH = 7.03), and 1% $NaHCO_3$ (pH = 8.35) on the synthesized AgNP@Au base (Fig. 4(c), Fig. 4(d)). The results revealed that the signal intensity of the main characteristic peak was highest in neutral solutions (pH = 7) and decreased obviously in acidic or alkaline solutions. The results demonstrated that a neutral or weakly acidic environment can enhance the Raman scattering signal of pesticide molecules, which is consistent with the finding of Kang et al. [38]. A reasonable deduction is that under alkaline conditions, OH^- ions compete with Cl^- ions to adsorb the metal pillars on the SERS surface and form the inactive sites, which weaken the DTC adsorption orientation.

Since a monomeric free DTC such as thiram exhibits significant SERS intensity, we hypothesized that adding EDTA to decompose the metal-DTC complexes would increase the SERS spectral intensity. This assumption may be verified by adding different concentrations of EDTA (0.01, 1, and 10 mM) to 10 ppm mancozeb solutions. To verify this assumption, EDTA (0.01, 1, and 10 mM) was added to the 10 ppm mancozeb solutions (Fig. 4(e)). The intensity of the main characteristic peak (1142 ± 5 cm^{-1}) of 10 ppm mancozeb solutions (equivalent to 40 mM) reached three thousand activity units (a.u.), which increased with the addition of EDTA. Fig. 4(f) showed that for 40 mM mancozeb, the enhancement of the main characteristic peak at 1142 cm^{-1}, when mixed with an equimolar amount of EDTA, is approximately 7-fold that in the absence of EDTA. However, given that 1 mM EDTA was added to 4 mM thiram, the SERS signal strength was not enhanced.

When more Zn and Mn ions in the mancozeb molecules were chelated by EDTA, the stability of the entire molecular structure might decrease and cause the molecular structure to collapse and ionize into disulfide amino acid monomers. More monomers would then combine with the SERS surface to scatter more Raman signals. Such a phenomenon also occurred in 10 ppm propineb mixed with 1 mM EDTA. It was noted that once EDTA was added, the band at 1045 cm^{-1} appeared in

Table 1
Extraction recovery rates for the incurred samples soaked in DTCs.

Incurred sample preparation[1]	GC-FPD (n = 5)		SERS (n = 5)			Recovery (%)
	DTC solution	[CS_2] (ppm)	Intensity ($\times 10^3$ a.u.)	[DTC] (ppm)	[CS_2][2] (ppm)	
Romaine lettuce soaked in 40 ppm DTCs	Thiram	0.32 ± 0.03	312	1	0.21	**65**
	Propineb	0.27 ± 0.07	11.5	2	0.4	**117**
	Mancozeb	0.59 ± 0.06	10.6	2.5	0.15	**78**
Romaine lettuce soaked in 80 ppm DTCs	Propineb	0.64 ± 0.05	18.3	4.5	0.86	**134**
	Mancozeb	0.85 ± 0.08	19.7	5	0.28	**111**
Broccoli soaked in 40 ppm DTCs	Thiram	0.12 ± 0.02	305	0.5	0.11	**88**
	Propineb	0.93 ± 0.08	30.6	7	1.21	**130**
	Mancozeb	0.97 ± 0.10	50.3	5	0.93	**97**

[1] Incurred samples were prepared by immersion in 40 ppm or 80 ppm DTC solution for 10 min followed by placement outdoors under sunlight for 2 h. CS_2 content was then quantified by GC-FPD.
[2] The concentration of CS_2 was calculated from the residual DTC content on the sample surface determined by SERS intensity, which involved a conversion factor. [CS_2] = [DTCs]/conversion factor.

the SERS spectra of thiram. The ethylenecarbamate [$(CH_3)_2NHCS_2$] moiety of thiram bound to the SERS surface should be free; therefore, both ν(C–S) and ν(C = S) modes were observed, displaying bands at 933 cm^{-1} and 1045 cm^{-1}, respectively. This outcome is indeed a troublesome situation in which the characteristic band observed at 1045 cm^{-1} interfered with the recognition of PBDC or EBDC residues. The results indicated that the addition of EDTA for SERS analysis was not appropriate, even though adding EDTA can facilitate the dissolution of residual DTCs on the surface of fruits and vegetables. The detection limit of this SERS method has reached the legal limit, even far below the MRL by tenfold. Thus, there is no need to add EDTA as an enhancer.

3.4. Detection limit and extraction efficiency

The optimized conditions obtained in the foregoing tests were used to determine the DMDCs (thiram and ferbam), EBDCs (mancozeb, maneb, and mitram), and PBDCs (propineb). The linear standard curves of these three types of DTC standard solutions are presented in Fig. 5 and Table S1. The lowest points of the standard curves were as follows: 2 ppb (equivalent to 8×10^{-9} M) for thiram, 0.1 ppm for propineb, and 0.2 ppm for mancozeb. All of these values were below the residue tolerance level of cabbage (2.5 ppm) stipulated by the Taiwan government. (CS_2 was used to determine the LOD of thiram for the instrument employed in the present study.) By using conversion factors, this study revealed that the LODs of CS_2 were as follows: thiram, 1.26 ppb; propineb, 0.05 ppm; and mancozeb, 0.06 ppm. These values were lower than the lowest residue tolerance level of DTCs (0.1 ppm) stipulated by the European Union for all crops. Compared with the LOD of a SERS method used for detecting thiram in previous studies, the LOD of 8×10^{-9} M in this study was better than that attained with silver supports such as nanowires (10^{-7} M) [43], silver nanoparticle–PDMS film (10^{-8} M) [44], silver nanoshells (10^{-8} M) [45], and nano-gold-based Au@Ag nanorods (1.5×10^{-7} M) [23]. Additionally, the LOD of this study was similar to that of materials combining nano-gold and nano-silver, such as Au@Ag nanoparticles (10^{-9} M) [46], Ag nanoparticles on a Au film over a nanosphere substrate (10^{-9} M) [30], and PNIPAM@Au nanorods (10^{-9} M) [47]. Although higher sensitivity of some SERS substrates has been declared [48,49], the associated procedures of chip fabrication or detection are more complicated and time consuming than the method we proposed in this study. In addition, considering the interference matrix in real samples, the method detection limit (MDL) should be higher than the LOD. For example, using multibranched gold nanostars, Zhu *et al.* (2018) reported that the LOD for thiram on apple peel samples was 0.24 ng/cm^2, which indicated that at least 0.24 ng of thiram can be determined in the matrix [50]. In contrast, we can determine 7.5×10^{-5} ng of thiram (0.05 ppm in a 1.5-μL extract) in a bok choy sample containing endogenous sulfur compounds. Therefore, the method proposed in this study had excellent performance in terms of the LOD for real samples. Liquid chromatography-tandem mass spectrometry (LC-MS/MS) can accurately detect and quantify the amount of DTC residues in vegetables and fruits (the LOD is approximately 10^{-10} M), but it involves a complicated procedure [51-54]. In contrast, the advantage of SERS is that the operation is simple and fast; the detection time of this method is less than 10 min, the LOD of SERS for thiram can reach the level of LC-MS/MS, and that for mancozeb was 3×10^{-4} ng, significantly lower than the value of 60 ng reported in a previous study [20]. Regarding propineb, no study reported its LOD determined by SERS. Therefore, this study first proposed distinguishing three molecular structure types of DTCs using SERS determination with an LOD comparable to the sensitivity of LC-MS/MS. As far as we know, apart from the detection method we proposed using SERS, there is no simple approach as an alternative or auxiliary method for the LC-MS/MS method to simultaneously distinguish DTCs such as DMDCs, EBDCs, and PBDCs on various crops.

For detection methods, the effective extraction of targets is another issue worthy of attention. Because DTCs are contact pesticides rather than nonsystemic pesticides, they mostly disperse across the surfaces of crops after being sprayed. Hence, extraction can be performed using a surface rinse method. To avoid drastic and rapid dissolution of DTCs in the plant tissue and consequential quantitative reduction, homogenization of the samples is not always necessary [55]. Moreover, the homogenization of samples engenders more coextracted substances, which interferes with determination. According to the results shown in Table 1, the efficiency of extracting DTCs by rinsing the surface exceeded 65%. Notably, the extraction efficiency of propineb (greater than130%) was higher than that of the other two types of DTCs, which may be due to the instability of the methyl substituents in propineb; however, this result does not mean that propineb was easier to extract by water. The extract solution with a weight equal to one-third that of the samples and a recovery ratio of 50% were conservatively used to calculate the MDL. For mancozeb, with the LOD of 0.2 ppm, the MDL in romaine lettuce was 0.13 ppm [= (0.2)*(1/3)*(1/0.5)], which was equivalent to 0.074 ppm CS_2 and meets the requirement of an LOD of 0.1 ppm CS_2 by GC-FPD analysis in most countries. Additionally, the MDL of thiram reached 1.3 ppb (equivalent to 5×10^{-9} M), which was far below the above mentioned requirement. Broccoli was used as a material to test for endogenous sulfur compounds. After washing the broccoli samples with water, GC-FPD analysis still detected an average CS_2 level of 0.22 ppm for five CK samples. However, no characteristic DTC signal was observed in the SERS spectrum of all 5 CK broccoli samples. This result showed that compared with GC-FPD, SERS had no false-positive results of DTC residues for crops containing glucosinolates or other sulfur compounds. Therefore, the method proposed in this study exhibited fairly reliable results in terms of quantitation limits and stability, regardless of whether the vegetables contained a high content of endogenous sulfur compounds.

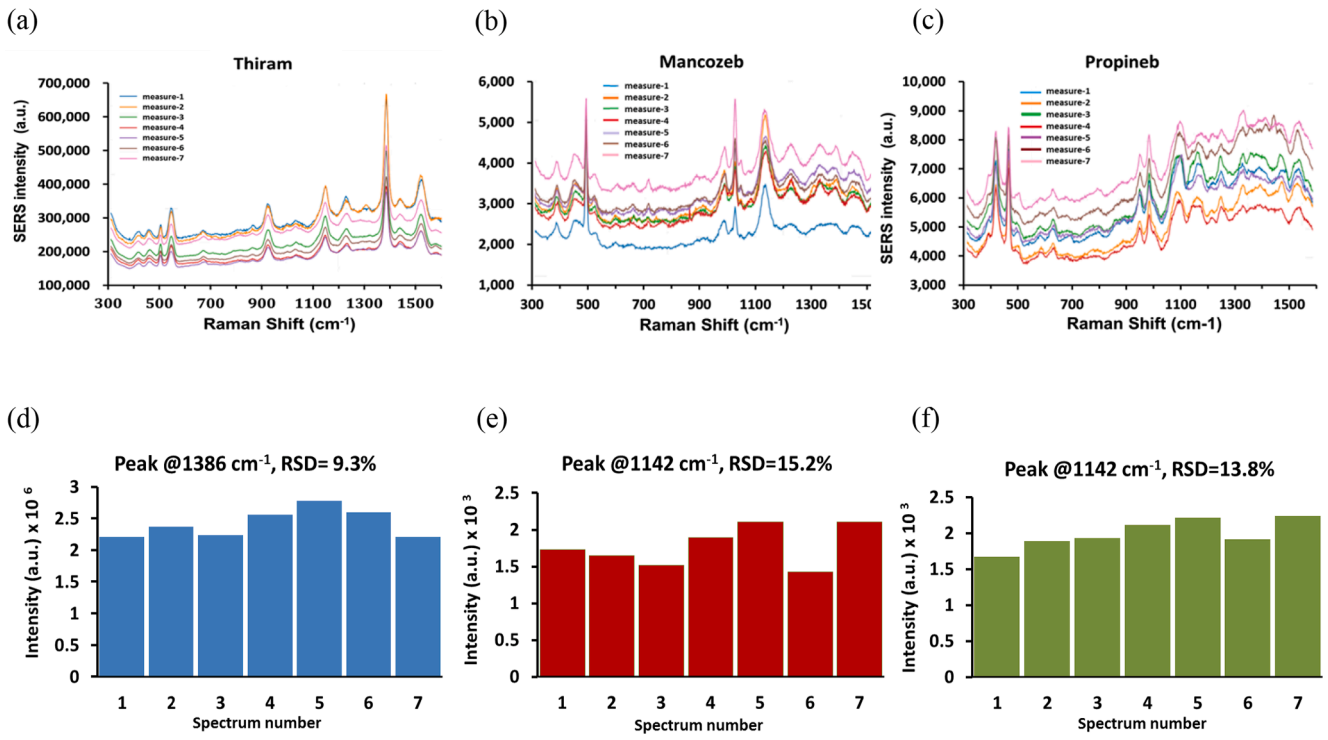

Fig. 6. SERS spectra of three DTC formulated pesticides in the extract of bok choy. The SERS spectra of (a) thiram (0.05 mg/L), (b) mancozeb (0.2 mg/L) and (c) propineb (0.1 mg/L), and the repeat stability of seven random measurements of intensity at (d) 1386 cm^{-1}, (e) 1142 cm^{-1} and (d) 1142 cm^{-1}.

3.5. Detection of formulated DTC pesticides in the matrix of real samples

It is well known that during the formulation or spray process, some additives are added to pesticides as adjuvants to enhance the stability, safety, convenience and anti-insect power of the active ingredient, such as emulsifiers, defoamers, spreaders, stickers, compatibility agents, and attractants. For instance, the commercial DTC formulation of WPs is a finely ground formulation with a particle size of approximately 5 μm containing 50–80% technical powder, 15–45% filler, 1–10% dispersant, and 3–5% surfactant [56]. These ingredients are mixed with water and applied to foliage as a standard insecticidal spray for ultralow volume or hydraulic applications. Therefore, we expect that the DTC residues on fruits and vegetables could be easily extracted with water. Through 0.45-mm membrane filters, DTCs dissolved in the extracts were passed, and other matrix particles were retained on the filter membrane. Fig. 6 (a)-(c) showed the SERS spectra after spiking the formulated agro-pesticide at 0.05, 0.2, or 0.1 ppm in an extract of bok choy and filtering the mixture. The characteristic peaks of the DTC formulated agro-pesticide were at constant positions when compared with those of the DTC reference standard. Moreover, in the extract solution of bok choy, distinctive and stable signs of characteristic peaks were observed through seven repeated determinations of DTCs at low concentrations. The results of this study indicated that our proposed approach exhibited excellent stability (relative standard deviation (RSD) < 16%), even in a real sample.

4. Conclusions

In summary, we successfully established a simple fabrication of Ag/Au alloyed nanopillars and applied the nanostructure as a SERS substrate to detect DTC residues in vegetables and fruits. The detection method only required water to extract most of the DTC residues on the surface of crops, avoiding the use of derivatizing reagents or reducing agents. The results showed that this approach was rapid, simple, safe, environmentally friendly and inexpensive. Furthermore, this Ag/Au alloyed nanostructure substrate for the SERS spectrum can distinguish DTCs comprising three different molecular structures, namely, DMDCs, EBDCs and PBDCs, which exhibit different toxicities. The excellent sensitivity of this method was 0.05, 0.2 and 0.1 ppm for DMDC, EBDC and PBDC compounds, respectively, and all met the requirements of the detection limit for DTCs in most countries. This study proposed a method that can provide a new auxiliary approach for existing DTC analysis methods to confirm excessive CS_2 in GC-FPD analysis and avoid false positive detection of endogenous sulfur-containing compounds (such as cruciferous leafy vegetables, mushrooms, and radishes).

CRediT authorship contribution statement

Chao-Ming Tsen: Methodology, Project administration, Writing - original draft. **Ching-Wei Yu:** Conceptualization, Software, Resources. **Sz-Ying Chen:** Formal analysis, Validation. **Cheng-Li Lin:** Investigation, Resources. **Chun-Yu Chuang:** Supervision, Writing - review & editing.

Declaration of Competing Interest

The authors declare that they have no known competing financial interests or personal relationships that could have appeared to influence the work reported in this paper.

Acknowledgements

This study was funded by the Council of Agriculture, Executive Yuan, Taiwan (grant No. 109AS-13.2.1-PI-P1) and the Ministry of Science and Technology, Taiwan (grant No. MOST 108-3111-Y-225-008). The authors thank Mr. Chi-Yi Lee, the Microscope Core Laboratory, Agricultural Chemicals & Toxic Substances Research Institute, Council of Agriculture, Taiwan, for recording the SEM images.

Ethical approval

This article does not contain any studies with human participants or

animals performed by any of the authors.

Informed Consent

Not applicable.

Appendix A. Supplementary material

Supplementary data to this article can be found online at https://doi.org/10.1016/j.apsusc.2021.149740.

References

[1] The International Agency for Research on Cancer (IARC), IARC Monographs on the Evaluation of Carcinogenic Risks to Humans, 2001, pp. 659–690.
[2] WHO, Ethylenethiourea (ETU) (Pesticide residues in food: 1993 evaluations Part II Toxicology), WHO, Geneva, 1993. Available from URL:http://www.inchem.org/documents/jmpr/jmpmono/v93pr08.htm.
[3] WHO, Propylenethiourea (PTU) (Pesticide residues in food: 1993 evaluations Part II Toxicology). WHO, Geneva, 1993. Available from URL:http://www.inchem.org/documents/jmpr/jmpmono/v93pr17.htm.
[4] G. Vettorazzi, W.F. Almeida, G.J. Burin, R.B. Jaeger, F.R. Puga, A.F. Rahde, F.G. Reyes, S. hvartsman, International safety assessment of pesticides: Dithiocarbamate pesticides, ETU, and PTU—A review and update, Teratogen Carcinogen Mutagen. 15 (1995) 313–337.
[5] Commission Directive 2007/57/EC of 17 September 2007.
[6] G.E. Keppel, Collaborative study of the determination of the dithiocarbamate residues by a modified carbon disulfide evolution method, J. Assoc. Off. Anal. Chem. 54 (1971) 528–532.
[7] D. Eloisa, H. Maria, C. Maria, K.R. Luiz, F. Joaquim, Determination of dithiocarbamate fungicide residues in food by a spectrophotometric mMethod using a vertical disulfide reaction system, J. Agric. Food Chem. 49 (2001) 4521–4525.
[8] V. Zisis, N. Emmanouil, P. Euphemia, Microwave-Assisted Extraction (MAE)−Acid hydrolysis of dithiocarbamates for trace analysis in tobacco and peaches, J. Agric. Food Chem. 50 (2002) 2220–2226.
[9] M. Nakamura, S. Noda, M. Kosugi, N. Ishiduka, K. Mizukoshi, M. Taniguchi, S. Nemoto, Determination of dithiocarbamates and milneb residues in foods by gas chromatography-mass spectrometry, Food Hyg. Saf. Sci. 51 (2010) 213–219.
[10] B. Denise, C. Paulo, M. Helio, Improvement in the determination of mancozeb residues by the carbon disulfide evolution method using flow injection analysis, J. Agric. Food Chem. 47 (1999) 212–216.
[11] J. Chang, H. Li, T. Hou, F. Li, Paper-based fluorescent sensor for rapid naked-eye detection of acetylcholinesterase activity and organophosphorus pesticides with high sensitivity and selectivity, Biosens. Bioelectron. 86 (2016) 971–977.
[12] X. Liu, M. Song, T. Hou, F. Li, Label-free homogeneous electroanalytical platform for pesticide detection based on acetylcholinesterase-mediated dna conformational switch integrated with rolling circle amplification, ACS Sens. 2 (2017) 562–568.
[13] X. Li, X. Gao, P. Gai, X. Liu, F. Li, Degradable metal-organic framework/methylene blue composites-based homogeneous electrochemical strategy for pesticide assay, Sens. Actuators, B 323 (2020), 128701.
[14] R.C. Perz, H.V. Lishaut, W. Schwack, CS2 blinds in brassica crops: false positive results in the dithiocarbamate residue analysis by the acid digestion method, Agric. Food Chem. 48 (2000) 792–796.
[15] J.K. Pandya, H. Dai, L. He, An innovative filtration based Raman mapping technique for the size characterization of anatase titanium dioxide nanoparticles, Talanta 224 (2021), 121836.
[16] H. Zhou, J.K. Pandya, Y. Tan, J. Liu, S. Peng, J.L. Muriel Mundo, L. He, H. Xiao, D. J. McClements, Role of mucin in behavior of food-grade TiO_2 nanoparticles under simulated oral conditions, J. Agric. Food Chem. 67 (2019) 5882–5890.
[17] H. Guo, Z. Zhang, B. Xing, A. Mukherjee, C. Musante, J.C. White, L. He, Analysis of silver nanoparticles in antimicrobial products using Surface-Enhanced Raman Spectroscopy (SERS), Environ. Sci. Technol. 49 (2015) 4317–4324.
[18] P. Wang, S. Pang, J. Chen, L. McLandsborough, S.R. Nugen, M. Fanb, L. He, Label-free mapping of single bacterial cells using surface-enhanced Raman spectroscopy, Analyst. 141 (2016) 1356–1362.
[19] S. Pang, T. Yang, L. He, Review of surface enhanced Raman spectroscopic (SERS) detection of synthetic chemical pesticides, TrAC Trends Anal. Chem. 85 (Part A) (2016) 73–82.
[20] P.A. Atanasov, N.N. Nedyalkov, Ru. Nikov, N. Fukata, W. Jevasuwan, T. Subramani, D. Hirsch, B. Rauschenbach, SERS of insecticides and fungicides assisted by Au and Ag nanostructures produced by laser techniques, Int. J. Environ. Agric. Res. (IJOEAR) 3 (2017) 61–69.
[21] P.A. Atanasov, N.N. Nedyalkov, N. Fukata, W. Jevasuwan, T. Subramani, M. Terakawa, Y. Nakajima, Surface-Enhanced Raman Spectroscopy (SERS) of mancozeb and thiamethoxam assisted by gold and silver nanostructures produced by laser techniques on paper, Appl. Spectrosc. 73 (2019) 313–319.
[22] M. Chen, W. Luo, Q. Liu, et al., Simultaneous in situ extraction and fabrication of surface-enhanced Raman scattering substrate for reliable detection of thiram residue, Anal. Chem. 90 (2018) 13647–13654.
[23] Y.Z. Zhang, Z.Y. Wang, L. Wu, Y.W. Pei, P. Chen, Y.P. Cui, Rapid simultaneous detection of multi-pesticide residues on apple using SERS technique, Analyst. 139 (2014) 5148–5154.
[24] M. Qi, X. Huang, Y. Zhou, L. Zhang, Y. Jin, Y. Peng, H. Jiang, S. Du, Label-free surface-enhanced Raman scattering strategy for rapid detection of penicilloic acid in milk products, Food Chem. 197 (Pt A) (2016) 723–729.
[25] Y.S. Li, J.S. Church, Raman spectroscopy in the analysis of food and pharmaceutical nanomaterials, J Food Drug Anal. 22 (2014) 29–48.
[26] P. Eiamchai, C. Chananonnawathorn, M. Horprathum, V. Patthanasettakul, S. Limwichean, N. Nuntawong, Spatial elemental investigations in nanostructured alloyed Ag/Au SERS substrates by magnetron sputtering oblique-angle co-deposition towardsincreased performance and shelf life, Appl. Surf. Sci. 513 (2020), 145748.
[27] S.K. Srivastava, A. Shalabney, I. Khalaila, C. Grüner, B. Rauschenbach, I. Abdulhalim, SERS biosensor using metallic nano-sculptured thin films for the detection of endocrine disrupting compound biomarker vitellogenin, Small. 10 (2014) 3579–3587.
[28] B. Saute, R. Premasiri, L. Ziegler, R. Narayanan, Gold nanorods as surface enhanced Raman spectroscopy substrates for sensitive and selective detection of ultra-low levels of dithiocarbamate pesticides, Analyst. 137 (2012) 5082–5087.
[29] B.N. Khlebtsov, V.A. Khanadeev, E.V. Panfilova, D.N. Bratashov, N.G. Khlebtsov, Gold nanoisland films as reproducible SERS substrates for highly sensitive detection of fungicides, ACS Appl. Mater. Interfaces. 7 (2015) 6518–6529.
[30] K. Guo, R. Xiao, X. Zhang, C. Wang, Q. Liu, Z. Rong, L. Ye, S. Chen, Silver nanopartical over AuFON substrate for enhanced raman readout and their application in pesticide monitoring, Molecules 20 (2015) 6299–6309.
[31] Y. Zhang, C. Yang, B. Xue, Z. Peng, Z. Cao, Q. Mu, L. Xuan, Highly effective and chemically stable surface enhanced Raman scattering substrates with flower-like 3D Ag-Au hetero-nanostructures, Sci Rep. 8 (2018) 898.
[32] Z.Q. Cheng, Z.W. Li, R. Yao, K.W. Xiong, G.L. Cheng, Y.H. Zhou, X. Luo, Z.M. Liu, Improved SERS performance and catalytic activity of dendritic Au/Ag bimetallic nanostructures based on Ag dendrites, Nanoscale Res Lett. 15 (2020) 117.
[33] Reasoned opinion of EFSA prepared by the Pesticides Unite (PRAPeR) on the modification of the existing MRL for dithiocarbamates, expressed as CS2, in garlic, EFSA Scientific Report 237 (2009) 1–40.
[34] C.M. Tsen, C.W. Yu, W.C. Chuang, M.J. Chen, S.K. Lin, T.H. Shyu, Y.H. Wang, C. C. Li, W.C. Chao, C.Y. Chuang, A simple approach for the ultrasensitive detection of paraquat residue in adzuki beans by surface-enhanced Raman scattering, Analyst. 144 (2019) 426–438.
[35] A.K. Samal, L. Polavarapu, S. Rodal-Cedeira, L.M. Liz-Marzan, J. Perez-Juste, I. Pastoriza-Santos, Size tunable Au@Ag core–shell nanoparticles: synthesis and Surface-Enhanced Raman Scattering properties, Langmuir 29 (2013) 15076–15082.
[36] Y. Yang, Q. Zhang, Z.W. Fu, D. Qin, Transformation of Ag nanocubes into Ag–Au hollow nanostructures with enriched Ag contents to improve SERS activity and chemical stability, ACS Appl. Mater. Interfaces. 6 (2014) 3750–3757.
[37] S. Sánchez-Cortés, M. Vasina, O. Francioso, J.V. García-Ramos, Raman and surface-enhanced Raman spectroscopy of dithiocarbamate fungicides, Vib. Spectrosc. 17 (1998) 133–144.
[38] J.S. Kang, S.Y. Hwang, C.J. Lee, M.S. Lee, SERS of dithiocarbamate pesticides adsorbed on silver surface; Thiram, Bull. Korean Chem. Soc. 23 (2002) 1604–1610.
[39] T.Y. Koh, SERS of dithiocarbamates and xanthates, Spectrochim. Acta Part A Mol. Biomol. Spectrosc. 51 (1995) 2177–2192.
[40] S. Sánchez-Cortés, C.Domingo, J.V. Garcia-Ramos, J.A. Aznarez, Surface-Enhanced Vibrational Study (SEIR and SERS) of dithiocarbamate pesticides on gold films, Langmuir. 17 (2001) 1157–1162.
[41] H.E. van Hart, H.A. Scheraga, J, Raman spectra of strained disulfides. Effect of rotation about sulfur-sulfur bonds on sulfur-sulfur stretching frequencies, Phys. Chem. 80 (1976) 1823–1832.
[42] M. Honda, M. Komura, Y. Kawasaki, T. Tanaka, R. Okawara, Infra-red and PMR spectra of some organotin(IV) N, N-dimethyldithiocarbamates, J. Inorg. Nucl. Chem. 30 (1968) 32321–33237.
[43] L. Zhang, B. Wang, G. Zhu, X. Zhou, Synthesis of silver nanowires as a SERS substrate for the detection of pesticide thiram, Spectrochim Acta A Mol Biomol Spectrosc. 133 (2014) 411–416.
[44] S. Liu, C. Jiang, B. Yang, Z. Zhang, M. Han, Controlled depositing of silver nanoparticles on flexible film and its application in ultrasensitive detection, RSC Adv. 4 (2014) 42358–42363.
[45] J.K. Yang, H. Kang, H. Lee, A. Jo, S. Jeong, S.J. Jeon, H.Y. Lee, D.H. Jeong, J. H. Kim, Y.S. Lee, Single-step and rapid growth of silver nanoshells as SERS-active nanostructures for label-free detection of pesticides, ACS Appl. Mater. Interfaces 6 (2014) 12541–12549.
[46] B.H. Liu, G.M. Han, Z.P. Zhang, R.Y. Liu, C.L. Jiang, S.H. Wang, M.Y. Han, Shell thickness-dependent Raman enhancement for rapid identification and detection of pesticide residues at fruit peels, Anal. Chem. 84 (2012) 255–261.
[47] Y.P. Wu, P. Li, B.H. Yang, X.H. Tang, Designing and fabricating composites of PNIPAM@Au nanorods with tunable plasmon coupling for highly sensitive SERS detection, Mater. Res. Bull. 76 (2016) 155–160.
[48] P.Z. Guo, D. Sikdar, X.Q. Huang, K.J. Si, W. Xiong, S. Gong, L.W. Yap, M. Premaratne, W. Cheng, Plasmonic core-shell nanoparticles for SERS detection of the pesticide thiram: size- and shape-dependent Raman enhancement, Nanoscale 7 (2015) 2862–2868.
[49] Y. Wang, Y.Y. Wang, H.L. Wang, M. Cong, W.Q. Xu, S.P. Xu, Surface-enhanced Raman scattering on a hierarchical structural Ag nano-crown array in different detection ways, Phys. Chem. Chem. Phys. 17 (2015) 1173–1179.

[50] J. Zhu, M.-J. Liu, J.-J. Li, X. Li, J.-W. Zhao, Multi-branched gold nanostars with fractal structure for SERS detection of the pesticide thiram, Spectrochimica Acta Part A: Mol. Biomol Spectrosc. 189 (2018) 586–593.
[51] G. Crnogorac, W. Schwack, Determination of dithiocarbamate fungicide residues by liquid chromatography/mass spectrometry and stable isotope dilution assay, Rapid Commun Mass Spectrom. 21 (2007) 4009–4016.
[52] G. Crnogorac, S. Schmauder, W. Schwack, Trace analysis of dithiocarbamate fungicide residues on fruits and vegetables by hydrophilic interaction liquid chromatography tandem mass spectrometry, Rapid Commun Mass Spectrom. 22 (2008) 2539–2546.
[53] B. Schmidt, H.B. Christensen, A. Petersen, J.J. Sloth, M.E. Poulsen, Method validation and analysis of nine dithiocarbamates in fruits and vegetables by LC-MS/MS, Food Addit. Contam. Part A Chem. Anal. Control Expo. Risk Assess. 30 (2013) 1287–1298.
[54] A. Kakitani, T. Yoshioka, Y. Nagatomi, K. Harayama, A rapid and sensitive analysis of dithiocarbamate fungicides using modified QuEChERS method and liquid chromatography–tandem mass spectrometry, J. Pestic. Sci. 42 (2017) 145–150.
[55] G. Crnogorac, W. Schwack, Residue analysis of Dithiocarbamate fungicides, Trends Anal. Chem. 28 (2009) 40–50.
[56] H.D. Burges, Formulation of Microbial Biopesticide, Kluwer Academic Publish, Dordrecht, The Netherlands, 1998, pp. 501–509.